Miniaturization of Electrochemical Detection System for Biuret-Based Peptide Detection Following Capillary HPLC

by

Xiaomi Xu

B.S. in Chemistry, Xiamen University, 2001

Submitted to the Graduate Faculty of

Arts and Sciences in partial fulfillment

of the requirements for the degree of

Master in Analytical Chemistry

University of Pittsburgh

2008

UNIVERSITY OF PITTSBURGH

ARTS AND SCIENCE

This thesis was presented

by

Xiaomi Xu

It was defended on

November 19, 2006

and approved by

Stephen G. Weber, Professor, Departmental of Chemistry

Shigeru Amemiya, Assistant Professor, Department of Chemistry

Adrian Michael, Associate Professor, Department of Chemistry

Thesis Director: Stephen G. Weber, Professor, Departmental of Chemistry

Miniaturization of Electrochemical

Detection System for Biuret-Based Peptide Detection Following Capillary HPLC

Xiaomi Xu, M.S.

University of Pittsburgh, 2008

Miniaturization of liquid chromatography, capillary HPLC, has made possible the separation of samples with volumes in the low microliter to nanoliter range. Downsizing separation column requires more sensitive detection method. Biuret-based electrochemistry has proven to be effective in peptide detection, but work needs to be done to make it feasible in capillary separation system.

This thesis presents modifications of a standard electrochemical detector with dual working electrodes, which decreases bandspreading into the nL range suitable for capillary HPLC. This miniaturized detector has detection limit of 3 nM (6 fmol) for peptides on the upstream anode. The downstream cathode has high selectivity by applying reductive potential. The common carbon working electrode can be replaced with gold electrodes with a self-assembled naphthalenethiol monolayer, which suppresses the background current from Au while giving detectable current from Cu-peptide redox reaction. When the modified Au electrode is assembled to a flow cell for peptide detection, it gives stable current response and the sensitivity is comparable to a glassy carbon electrode.

These advances will permit non-electrochemists to determine peptides by capillary HPLC quantitatively, and open the way for chip-based detectors.

TABLE OF CONTENTS

LIST OF TABLES

LIST OF FIGURES

PREFACE

I would like to express my deep and sincere gratitude to my supervisor Dr. Stephen G. Weber, whose help, stimulating suggestions and encouragement helped me in all the time of research. He always emphasizes the importance of being an independent and creative researcher, which is very crucial for both current pursuit of Master degree and the future research career.

I thank Dr. Amemiya and Dr. Michael as my committee. Their great knowledge in analytical chemistry and biochemistry is very helpful in my learning and research work.

I want to thank Weber group for all their help, support, interest and valuable hints. The discussion with Dr. Zudans helps me a lot in understanding the research work and making progress. Hongjuan Xu is kind enough to prepare rat brain slice for my biological sample extract experiment.

I thank Mattias Tranberg for his instruction of preparing sample extract through E-mail communication. I thank Tom from machine shop who gave me help with making flow cell electrode block.

1.0 INTRODUCTION

1.1 PEPTIDE DETERMINATION USING HIGH PERFORMANCE LIQUID CHROMATOGRAPHY

Biochemical studies often depend on the analysis and characterization of minute amounts of proteins or peptides, or their metabolites, isolated from cell cultures or biological organisms. Peptides play a significant role in control and regulation of many vitally important processes in the living organisms. However, biological samples always contain very complicated matrix in that there are many different compounds with different concentrations. Therefore, highly sensitive and selective analytical methods are essential to accomplish accurate determination of peptides.

The introduction of high-performance liquid chromatography (HPLC) to the analysis of peptides and proteins revolutionized the biological sciences by enabling the rapid and sensitive analysis of peptide through the exquisite speed, sensitivity and resolution that can be easily obtained[1]. Among its various modes, reversed-phase high-performance liquid chromatography (RP-HPLC) involves the separation of molecules on the basis of hydrophobility. The separation depends on the hydrophobic binding of the solute molecule from the mobile phase to the immobilized hydrophobic ligands attached to the stationary phase, i.e., the sorbent. RP-HPLC is

extremely versatile for the isolation of peptides from a wide variety of synthetic or biological sources[2].

Some peptides exist in living organisms in very low concentration. For example, the total concentration of neuropeptides in mammalian brain is only a few micromolar[3]. And samples obtained from brain tissues are inevitably diluted during sampling procedures. Not only do neuroactive peptides exist in low concentration, the total volume is limited too. So besides the requirement in high concentration and mass sensitive detection, the miniaturization is also a desirable trend.

Microcolumn LC[4] (smaller than 1.0 mm in I. D.) has the ability to work with minute sample size and small volumetric flow-rates, featuring low reagent consumption and increased analytical performance[5, 6]. Capillary columns usually refer to the columns with internal diameter of 0.1 mm to 0.5 mm[7]. The material for capillary columns is mainly fused silica tubing with outer polyimide coating. Although the methods and instrumentations developed for conventional LC system should be applicable to the capillary LC, decreasing the column volume puts stringent requirements on the instrumentation: all volumetric extracolumn dispersion sources have to be scaled down, especially injection and detection.

Further miniaturization of the capillary separation systems leads to the concept of microchip separation, and furthermore, micro total analysis systems (μ-TAS), which is especially appealing to field analysis. While tremendous advances have been made in the miniaturization of capillary electrophoretic separation systems, the problems of microfabrication of an efficient μ-LC remain[8, 9], in particular the sealing of the μ-channels to allow the mobile phase to be pumped through chip at pressures exceeding 2000 psi and coupling to external instrumentation without leakage and without the introduction of dead volume[10].

One of the issues concerning size reduction of the separation system is the resulting demands on the detection system. For example, the sample volume in capillary LC is in a few microliters to nanoliters range, and can be less than 1 nL in microchip separation[11]. Therefore, very high sensitive detector should be constructed to analyze even modest concentration of sample solutions. Also, there is the need to miniaturize the detector size to achieve the ultimate goal of μ-TAS.

1.2 DETECTION IN MINIATURIZED LC SYSTEMS

In principle, conventional detection methods should be applicable to miniaturized LC system. However, some widely used detection techniques in conventional HPLC, for example, refractive index detection, are less common in miniaturized LC due to the low sensitivity. Some detection schemes that are common in both conventional and miniaturized LC systems are discussed here.

1.2.1 UV-vis absorbance

The most universally applied detector, in conventional and capillary LC, is UV absorbance detector because of its ease of use and broad application area. To prevent extracolumn band broadening, on-column detection scheme is often used in capillary LC system. This is accomplished by removing the protective polyimide coating from the silica capillary column after the frit to provide a detection window[12-14]. Because of the small-diameter capillaries used, however, the path length of these detection cells is very short and yields concentration detection limits of only 10^{-5} to10^{-6} M[15]. Also, problems involved in focusing and collecting light onto and

from the capillary have been limiting factors in the use of UV-vis absorbance for microseparations.

1.2.2 Laser induced fluorescence (LIF)

Fluorescence detection is very attractive among the various miniaturized detection techniques. Fluorescence emission provides more selectivity and the spectra can be utilized to reveal structural information of unknown compounds[16, 17]. Most common fluorescence detection scheme used in microcolumn LC deal with laser-induced fluorescence: light from a laser is focused onto an on-column window and accounts for the increased sensitivity of the technique. Although lasers offer a limited range of excitation wavelengths and samples typically need to be derivatized before or after separation to make them fluorescently active, LIF detection is still very attractive because of its low detection limits: routinely obtained mass detection limits are typically in the amol range[4]. Moreover, LIF is the most popular detection mode for microchip so far[11]. However, the large and expensive lasers and optics systems required for LIF detection is some way off from integration in chip.

1.2.3 Mass spectroscopy (MS)

MS is another detection scheme common in macroscale separations that has been applied to microcolumn separations, primarily in connection to proteomic analysis. This technique is attractive because of its general applicability and its ability to yield structural information. Coupling microcolumn to MS is not as straightforward as coupling to optical detection methods because the on-column scheme cannot be used. The introduction of continuous flow fast atom

bombardment and atmospheric pressure ionization techniques (electrospray ionization and atmospheric pressure chemical ionization) have contributed greatly to the current success of microcolumn LC-MS[4]. MS has also been used as a detection mode for chip[18, 19]. While it provides rich chemical information, MS has the same problems with LIF: its high cost and large size of the instrumental set-up make it incompatible with the concept of μ-TAS.

1.2.4 Electrochemical detection (ED)

Because of its ease of implementation, ability to selectively detect analytes, high sensitivity (approaching that of fluorescence) and its sensitivity independent of optical path length, EC is successful in both conventional and microcolumn LC. Unlike LIF or MS, EC features inherent miniaturization of both the detector and control instrumentation and is compatible with advanced micromachining and microfabrication technologies, which makes it extremely attractive as microchip separation detection scheme[20]. EC detection scheme of peptides and the detector cell design for miniaturized LC systems will be discussed.

1.3 DETECTION IN MINIATURIZED LC SYSTEMS

1.3.1 Biuret based peptide detection

LC-EC has provided a powerful tool for the determination of peptides in biological mixtures. Peptides containing electroactive amino acids, such as tyrosine, tryptophan, and cysteine can be detected directly through electrochemical method[21-23]. Peptides containing one or more primary

or secondary amines can be detected after derivatization with o-phthalaldehyde[24, 25] or 2, 3-naphthalenedialdehyde[26]. Of course, not all important peptides contain easily detected amino acids. Weber group[27, 28] developed a method using biuret reaction for the electrochemical detection of peptides that are not electroactive following their separation by HPLC. In this method, peptides react with Cu^{2+} under basic conditions to form a complex that can be detected electrochemically based on oxidation of Cu^{2+}-peptide to Cu^{3+}-peptide and reduction of Cu^{3+}-peptide to Cu^{2+}-peptide. This derivatization is unique in that the reaction does not require primary amines but rather involves the peptide backbone. As a result, the method is highly selective for peptides and allows detection of peptides, such as those with post-translational modifications to the N-terminus, which are undetectable by reagents that act on amines.

1.3.2 Dual electrode detection scheme in capillary LC

In electrochemical detection of peptides in complex biological samples, great selectivity is desired besides a judicious choice of the potential of the working electrode. Based on the reversibility of the biruet complex, this can be achieved by using dual-electrode systems. The use of a series dual electrode amperometric detector (upstream anode, downstream cathode) for the selective detection of bioactive peptides has been demonstrated[27].

However, dual electrode EC detector used in conventional LC is not suitable for capillary LC because of the inherent low flow rate and sample volume. There are relatively fewer reports about dual electrode detection in capillary LC, but research work in designing dual- or multi-electrode cell for capillary electrophoresis (CE) is plenty. We can refer to those cell designs used in CE-EC for capillary LC-EC. The difference is that the electrochemical detector needs to be

isolated from the separation voltage in CE-EC, which is realized either by using a decoupler in off-column detection or by using small-diameter capillaries in end-column detection[29].

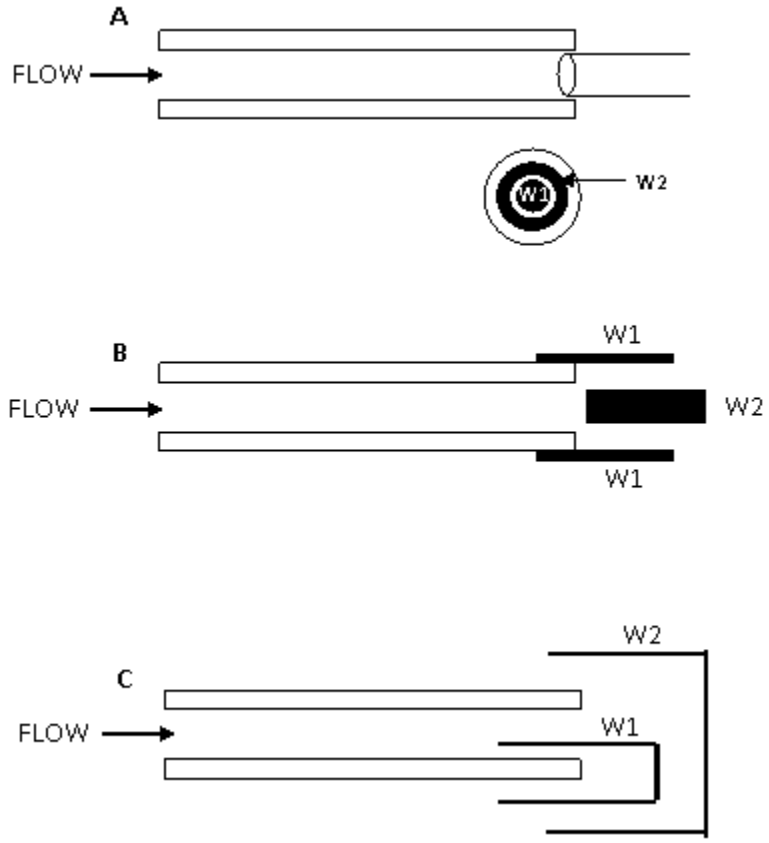

Figure 1 Dual-electrode configurations for CEEC

A. ring-disk, B. tubular-wire, and C. wire-wire

The first reported dual electrode detector for CE is fabricated by inserting a generator electrode in a capillary through small holes drilled in the capillary and aligning a collector electrode at the outlet[30]. Some more dual electrode designs are shown here (Figure 1). Figure 1A shows a micro ring disk electrode design[31], consisting of a carbon fiber disk electrode and chemical vapor deposited carbon ring electrode. Zhong and Lunte[32] described a dual electrode detector consisting of a gold tube and a wire inserted into the capillary (Figure 1B). The third

design developed by Holland[33, 34] consisted of two wires at the end of the capillary, one inside the tube and a second across the end of the capillary (Figure 1C).

Although those designs include smart ideas, some of the fabrication processes are complicated, and a micropositioner and a microscope are needed to align the detector with the capillary end. Also, the detection limits are pretty high (several micromolars). More standard and sensitive dual electrode detectors are desirable for capillary LC.

1.3.3 EC in microchip separation

There are different methods in fabricating electrodes in the chip. The working electrode can be integrated directly on the chip or positioned external to the chip at the end of the separation channel. Although some research groups have reported externally positioned off-chip electrode alignment, most have chosen to incorporate the EC working electrode directly onto the chip[35]. Advantages to integrating the electrode directly on the chip include the fact that the electrodes are reproducibly made with the same photolithographic procedures that are used to make the separation component of the chip, meaning the chip is amenable to mass production. In addition, this approach also has the advantage that the specific electrode features critical for optimum detector performance (e.g., the number of electrodes and their exact size, shape, and placement) can be precisely controlled during chip fabrication.

Metal electrodes, including gold[36], platinum[37], copper[38], can be readily integrated on-chip using photolithographic procedure via sputtering or vapor deposition as an additional step in the microfabrication process. The carbon electrode fabrication usually involves inserting a carbon fiber[39] or carbon paste[40] into a microchannel on a polymer substrate and sealing it to another

polymer/glass substrate containing the separation channel network. With this approach, however, the electrodes are not microfabricated and therefore, not amenable to mass production.

Au electrodes have been used to detect a number of different analytes, including catechol[41-44], neurotransmitters[41-43], amino acids[45], carbohydrates[45-47], antibiotics[45], uric acid[46, 48], ascorbic acid[46] and DNA restriction fragments[44]. However, gold electrodes are generally less useful for the direct amperometric detection of many compounds due to the narrow electrochemical window and possible analyte irreversible adsorption. Therefore, better understanding of Au electrochemistry and appropriate surface treatment of Au are desired.

1.4 GOLD ELECTRODES

1.4.1 Bare Au electrochemistry

Gold electrodes have narrower electrochemical window compared to carbon because they tend to be oxidized easily especially in alkaline solution. The electrochemical window refers to the electrochemical potential range over which no redox reaction occurs considering either the solution species or the electrode surface. The electrochemical window of a carbon electrode basically depends on the solution species, while that of a gold electrode is confined by Au oxide formation on gold surface.

Based on the thermodynamic data[49], gold should be oxidized to the trivalent state, according to the reaction: $Au + 3H_2O \rightarrow Au_2O_3 + 6H^+ + 6e^-$ at 1.457 V vs. RHE if the product is the hydrated oxide (which may be represented as $Au(OH)_3$ or $Au_2O_3\ 3H_2O$), or at 1.511 V vs. RHE if the product is the anhydrous oxide[50]. But this value is estimated for the stable bulk metal

atoms and it is only in the case that μ(Au) = 0. Surface atoms are inevitably more active; the absence of similar metal neighbors on one side means that they are lacking some of the lattice stabilization energy of their bulk equivalents and, hence, they tend to oxidize at a lower potential.

Cyclic voltammetry (CV) is a widely used technique to study the electrode surface behavior in aqueous media. Typical cyclic voltammograms for gold in acid and base (Figure 2) show the increase in anodic current in the positive sweep, commencing at about 1.36 V vs. RHE in 1 M H_2SO_4 and 1.05 V in 1M NaOH The potential for the onset of oxidation decreased with increasing solution pH by a factor of about 30 mV/pH unit[51].

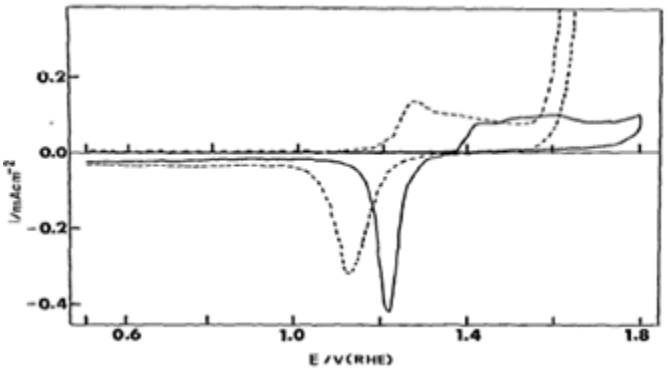

Figure 2 Typical gold voltammograms in acid and base solutions

Reprinted from [51], with permission from Elsevier.

The anodic response is not a single sharp peak, but a plateau, while monolayer oxide reduction expressed as a relative sharp cathodic peak with hysteresis. The complicated Au oxide formation CV properties are attributed to gradual changes in the nature of the oxide film. The early stage of oxidation of noble metal surfaces is usually discussed in terms of adsorbed hydroxy radical formation[52], $H_2O \rightarrow OH_{ads} + H^+ + e^-$. In the case of gold, the involvement of a hydroxy species is considered as some type of metal-hydroxy compound, e.g., $Au^{\delta+}\ldots OH^{\delta-}$, the product being a polar covalently-bonded species. During the growth process, dipolar ($Au^{\delta+}.OH^{\delta-}$) species repel one another. Such repulsion raises the energy required to generate additional

dipoles; hence, there is an increase in potential with increasing coverage. This is evidently the reason why the monolayer oxide formation response is an extended plateau rather than a sharp peak. In the negative sweep the dipole coverage (and any residual stress) is progressively reduced. No electrostatic repulsion barrier is developed in this case and a relative sharp cathodic peak is observed.

1.4.2 Au surface cleaning

As reported in the literature, an important factor in using solid electrodes is the dependence of the response (in terms of activity, stability and reproducibility) on the electrode surface conditions[53, 54]. Accordingly, the use of such electrodes requires precise and specific surface electrode pretreatment in order to obtain the aimed results. Especially in the context of surface modification, the properties of the gold substrate play an important role in the self-assembly process and on the properties of the resulting monolayer[55].

Polycrystalline gold electrodes are more attractive for analytical purposes than single crystalline ones owing to their practical handling[56]. Among many different procedures for cleaning and preparing polycrystalline Au surfaces, some of them have been extensively used in the last years, including mechanical, chemical and electrochemical pretreatments.

The mechanical pretreatment procedure consists of manually polishing the gold electrodes to mirror-finished with emery paper, alumina or diamond slurries. This is usually followed by chemical pretreatment procedure, dipping the gold electrode into fresh piranha solution (7/3 v/v concentrated H_2SO_4/H_2O_2), to remove organic absorbed materials. After these procedures, electrochemical steps, successive scans between gold redox potentials in 0.5 M H_2SO_4 aqueous solution, are commonly performed in order to create a smooth and active

electrode surface[57]. Although organic contaminants residues left by preceding cleaning treatments can be removed by repeated cycling of the electrode potential between limits at which gold is oxidized and reduced, electrochemical pretreatment is not appropriate to be applied alone at hydrostatic conditions as an effective cleaning step. For that reason electrochemical pretreatment is usually applied succeeding mechanical or chemical cleaning treatment.

1.4.3 Self-assembled monolayer (SAM) on Au

Self-assembled monolayer (SAM) refers to a single layer of molecules adsorbed spontaneously by chemisorption to the metallic surfaces such as Au, Ag, Pt, etc., to form a highly ordered surface with fewer defects and exhibit a high degree of orientation, molecular ordering and packing density[58]. SAM provides a means for controlling the chemical nature of the electrode solution interface.

Among numerous self-assembly systems, thiolates are probably the most commonly used system for SAM on gold. Most studies on film formation, structure and properties of SAM modified Au are based on aliphatic thiols. Electron transfer through aliphatic thiol SAM occurs with tunneling mechanism, which decays exponentially with the aliphatic chain length[59]. Aliphatic thiol monolayers essentially form an insulation layers between the gold substrate and the adjacent electrolyte, which inhibit not only gold oxide formation but charge transfer with redox systems within the electrolyte as well. Also, the thiolate headgroup of alkanethiol SAM is prone to oxidation under ambient conditions, forming sulfinates and sulfonates. These oxidized monolayers have compromised structural stability because they are no longer chemisorbed and can be washed away.

Aromatic thiol SAM has higher rigidity and higher electron transfer rate owing to the presence of delocalized π-electrons in the aromatic ring[60]. Moreover, when the mercapto group is directly attached to an aryl, the thiolate is less prone to oxidation under ambient conditions. Modification of Au surface with proper aromatic thiols can essentially broaden the electrochemical window by suppressing Au surface oxide formation, while promoting the electron transfer of the electroacitve species in the solution to the electrode.

1.5 PROPOSAL

Miniaturization of liquid chromatography, capillary liquid chromatography, has made possible the separation of samples with volumes in the low microliter to nanoliter range. Our lab has developed earlier the use of carbon fiber microelectrodes in conjuction with a copper-based postcolumn reagent for trace determination of peptides. However, carbon fiber-based detection works require a micromanipulator and microscope for proper positioning of the electrode. Further, the optimal detection mode is a series dual electrochemical detector with upstream oxidation and downstream reduction detection. This is virtually impossible with carbon fibers. Also, development of microfluidic devices with this chemistry is currently impractical – the electrochemistry does not work at metal electrodes (which are easy to make in the chip context) but carbon is hard to make in the chip context.

We propose to construct a miniaturized dual electrode detector for capillary LC by modifying a standard HPLC electrochemical detector. Also, we propose to replace the glassy carbon with gold electrodes with a self-assembled aromatic monolayer, which is supposed to suppress the background current from Au while giving detectable current from Cu-peptide redox

reaction. These studies are targeted to permit non-electrochemists to determine peptides by capillary HPLC quantitatively, and open the way for chip-based detectors.

2.0 OPTIMIZATION OF A DUAL ELECTRODE FLOW CELL FOR BIURET-BASED PEPTIDE DETECTION FOLLOWING CAPILLARY HPLC

2.1 INTRODUCTION

Capillary HPLC is advantageous in trace analysis because of the increased mass sensitivity that can be achieved with a smaller column volume[7]. The most common approach to electrochemical detection after capillary HPLC, also the detection scheme currently used in our lab's research work, utilizes a microelectrode, typically a cylindrical fiber or wire, inserted into the column outlet or postcolumn capillary reactor[61]. Although generally microelectrodes display high signal-to-noise ratio[62-64], they have several disadvantages, for example, carbon fibers, are easily broken upon handling and positioning in the capillary, the physical properties of every single carbon microelectrode vary which may cause irreducibility in detection current, and, dual or series working electrodes designs are almost impossible using this in-column configuration.

These problems lead to the thoughts of building a dual electrode end-column electrochemical detector, which uses solid electrode material, e.g., glassy carbon, gold. Thus, it will be easy to work with and have better reproducibility. However, end-column detector may cause loss of chromatographic efficiency due to extra-column band spreading. This is especially critical for miniaturized chromatographic systems[65] considering the associated small peak volumes.

We will start with adapting a commercial dual-electrode end-column electrochemical detector to the capillary format, focusing on reducing postcolumn volume and increasing signal-to-noise ratio. The performance of the flow cell will be examined and optimized following standard peptide sample flow injection and capillary HPLC. Biological samples extracted from rat brain slices will also be analyzed using our capillary HPLC-EC detection system, in which case shows the advantage of dual electrode detection.

2.2 EXPERIMENTAL

2.2.1 Reagents

Reagents and sources were as follows: acetonitrile (ACN) and trifluoroacetic acid (TFA), Sigma (St. Louis, MO); 1-propanol, disodium tartrate dihydrate and copper sulfate pentahydrate, J. T. Baker (Phillipsburgh, NJ); ACS grade sodium carbonate and sodium bicarbonate, Sigma-Aldrich; Tetraglycine (GGGG), leucine enkephalin (YGGFL), des-tyr leu enkephalin (GGFL), methionine enkephalin (YGGFM) and des-tyr met enkephalin (GGFM), BACHEM (King of Prussia, PA).

The copper sulfate pentahydrate was recrystallized from water. The disodium tartrate dihydrate was recrystallized from dilute NaOH. All other reagents were used without further purification.

All solutions were made with Milli-Q (Millipore, Billerica, MA) house-deionized water.

2.2.2 Flow injection

The aqueous flow solution containing 0.24 M $NaHCO_3$, 0.24 M Na_2CO_3, 12.0 mM Na_2Tar and 2.0 mM $CuSO_4$ was pumped with a Harvard Apparatus (Holliston, MA) pico plus syringe pump and 5 mL Hamilton (Reno, NV) Gas tight syringe. Three different flow rates were used: 10 μL/min, 15 μL/min and 20 μL/min. A VICI 6-valve injector from Valco Instrument (Houston, TX) was used for sample injection with an injection volume of 10 μL. The sample was prepared by adding GGGG to the flow solution (biuret reagent) with the final concentration of 10 μM Cu-GGGG.

Potential was controlled with a BAS (West Lafayette, IN) Epsilon LC potentiostat. An Ag/AgCl, 3 M NaCl (BAS, Model RE-5B) reference electrode was used and all the potentials were referred to it.

Data were imported into Origin 7.5 (OriginLab Corporation) for differentiation, then exported to PeakFit version 4 (AISN Software, Inc.) for determination of the first and second central moments, which represent time and the standard deviation, respectively. The statistical moments were determined by fitting the 5-parameter GEMG function to the data based on the least squares criterion[66].

2.2.3 Capillary liquid chromatography

The filtered (Osmonics, Minnetonka, MN) mobile phase containing 0.1 % TFA, 3% 1-propanol and 23% acetonitrile was pumped at 100 μL/min with a Waters 590 pump. To achieve the low flow rates used in capillary HPLC the mobile phase flow was split using a simple tee and provide a flow rate of 1 μL/min to the capillary column. The splitting ratio depends on the pressure on

both sides of the splitting tee. The waste line is calculated to be 12 cm × 25 μm (I.D.) when a 10 cm × 100 μm (I.D.) column packed with 2.6 μm particles is used. The biuret reagent was pumped at 0.3 μL/min with a Harvard Apparatus pico plus syringe pump.

Capillary columns were prepared by previously described techniques[3] using 20 cm lengths 100 μm ID, 360 μm OD fused silica capillaries as the column blanks. The 100 μm ID columns were slurry packed with 2.6 μm XTerra MS-C18 (Waters, Milford, MA) reversed-phase particles (slurries consisted of 20-30 mg/mL packing material in isopropanol) at 3000-4000 psi using a constaMetric III metering pump (LDC Analytical, Riveria Beach, FL).

Reactors construction procedure was developed in our lab[67]. Briefly, two 25 μm tungsten wires were each threaded through a 75 μm fused silica tube. After that, both ends were threaded through another 75 μm fused silica tube. A piece (~ 1.5 cm long) of dual shrink/melt tubing (Small parts, Miami Lakes, FL) was used to combine the junction between the three capillary tubes. After sufficient heat was applied with a heat gun (Wagner Spray Tech Corporation, Minneapolis, MN), the inner part of the tubing was melted while the outer part was shrinked. The tungsten wires were removed after the device was cooled down and fluid conduits were created within the polymer tube.

The injection and electrochemical detection parts were the same with those used in flow injection experiment, except that the injection volume here was 2 μL.

2.2.4 Sample preparation

Organotypic slice cultures of the hippocampus were prepared from the brains of six-day-old rats. The animals were decapitated and the hippocampus area was dissected. A McI1wain tissue chopper (the Mickle Laboratory Engineering Co. Ltd) was used to cut the hippocampus into

slices with desired thickness. Slices were separated in GBSS solution containing 2.7 mM $MgSO_4$ and 0.45% D-(+)-glucose under a microscope. The slices were then transferred to pre-cooled Eppendorf tubes and snap frozen in liquid nitrogen. To homogenize the tissue, 90% methanol in water (250 µL for four slices) was added and the tube was placed in an ice-bath and sonicated using Microso Ultrasonic cell disruptor XL 2000. To avoid overheating, the sample was sonicated for 3 seconds, and then allowed to cool down for 10 seconds. The procedure was repeated for about 5 times or until the whole solution turned opaque and there was no solid left. After storage at -20 ℃ overnight, the tubes were centrifuged at 11000 g using Jouan Centrifuger A-12 for 3 minutes. The supernatant was removed and filtered with 0.22 µm syringe filters (Millipore, Billerica, MA). Finally, the methanol was evaporated to dryness in a speed vacuum. 0.1 % TFA aqueous solution was added to the sample and vortexed for analysis.

The sample was also extracted with a ZipTip[68] (Millipore, Billerica, MA). A ZipTip is a pipette tip with a bed of chromatography media fixed at its end. Because our HPLC column was reversed-phase, we used the ZipTip containing a small amount of reversed phase packing material, C_{18}. ZipTip treatment is intended for concentrating and purifying peptides, protein or oligonucleotide samples. The ZipTip treatment was performed according to manufacturer specifications. The tip was wet with acetonitrile and equilibrated with 0.1% TFA. The sample components were then extracted by aspirating and dispensing the sample until it was completely eluted (typically 10-15 cycles). 0.1 % TFA solution was used to remove sample components not bound to the C_{18} reversed phase packing material. The bound sample components were eluted using 5 µL 50 % ACN/0.1 % TFA solution with 10-15 cycles. Samples were then diluted with 25 µL 0.1 % TFA.

2.3 RESULTS AND DISCUSSION

2.3.1 Examination of extra column band spreading

Our lab developed a simple method based on flow injection for the quantitative examination of extra column band broadening in microchromatographic systems[66]. In this method, a large sample loop is used to produce a steady-state signal that can be differentiated to yield two peaks. Based on the slope of the first and second central statistical moments (time t and standard deviation σ_t^2) of the peaks under different flow rates, one can decide the experimental plate height in units of time, "plate time", H_t. By comparing the theoretical with experimental values, one can decide whether there is significant band spreading in the system, which is believed to be mainly from the end-column flow cell. The flow cell is composed of a BAS auxiliary electrode, a 22 μm thick gasket with 1 mm wide flow channel and a working electrode block with two 1 mm

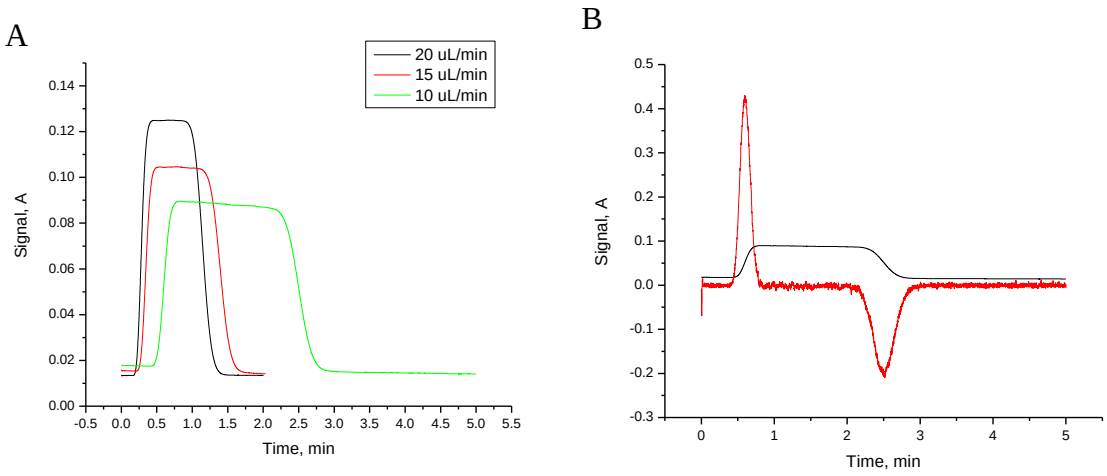

Figure 3 Flow injection and data analysis

(A) Flow injection analysis of 10 μM Cu-GGGG. (B) A data trace and the first derivative

diameter glassy carbon electrodes, but only the upstream anode (the first electrode) response is used in this section. Optimization of the cell design will further be discussed in Section 2.3.4.

Figure 3A shows the signal response at three different flow rates with an injection volume of 20 μL. Flow injection experiments are repeated at least three times for each flow rate. Differentiation of the signal response yields the first derivative of the data trace shown in Figure 3B. Sample injection generates a plateau with two steps, which are differentiated to yield two peaks. The following calculation is based on the first step and the corresponding derivative, because the second step includes the information of extra bandspreading caused by diffusion in the loop.

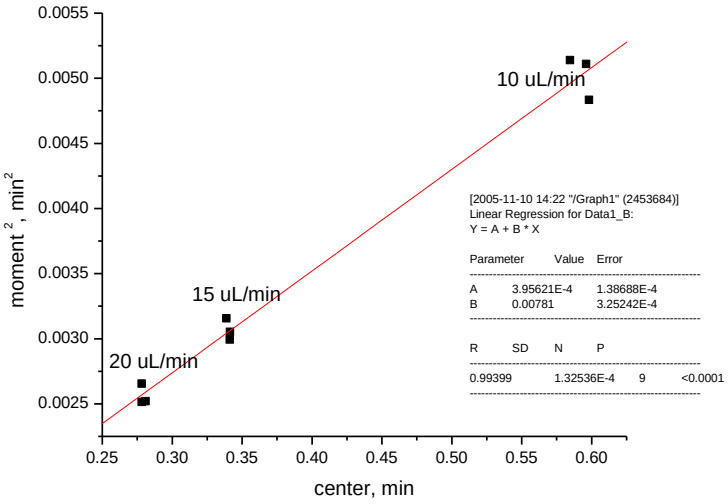

Figure 4 Relationship between second central moment and first central moment

The relationship between the first and the second moments is plotted in Figure 4. Linear fit of the data gives the equation, $y = 0.00781x + 0.00039, R^2 = 0.994$. The experimental value of the "plate time", H_t, is the slope, 0.00781.

The theoretical "plate time" can be calculated[66], $H_t = a^2 / 24D$. The capillary radius, a, is 75 μm. The diffusion coefficient, D, of Cu(II)-GGGG is found to be $(3.96 \pm 0.14) \times 10^{-6}$ cm^2/s in rotating ring-disk electrode study[69]. So based on these two values, a = 75 μm, D = 3.96×10^{-6} cm^2/s, the "plate time", H_t, is calculated to be 0.00986 min.

The theoretical value, 0.00986 min, and the experimental value, 0.00781 min, are pretty close. So there is some but not significant extra-column band spreading from the detector.

2.3.2 Using the dual electrode flow cell in capillary HPLC

2.3.2.1 GGFL

To validate the performance of the dual electrode flow cell in the EC detection of peptide after HPLC, des-tyr leu-enkephalin (GGFL) is used as the model system. Enkephalins, a type of neuropeptides, are peptides that we are interested in for understanding the brain chemistry. There are two types of enkephalins: Leu-enkephalin (YGGFL) and Met-enkephalin (YGGFM); GGFL and GGFM are their corresponding hydrolysis products. GGFL is used as the testing peptide here because its electrochemical detection on carbon electrodes has been well studied in our lab. Post-column reactor with biuret derivatization is connected before the detector, as GGFL is not electroactive itself.

Figure 5 shows the simple chromatogram of GGFL with concentration ranging from 0.1 μM to 1 μM. The potential on the upstream anode is set at 0.6 V vs. Ag/AgCl, oxidizing Cu(II)-GGFL to Cu(III)-GGFL. Cu(III)-GGFL is being reduced back to Cu(II)-GGFL on the downstream cathode, 0.1 V vs. Ag/AgCl. The peak width is quite similar to the results with the microelectrode under the same chromatographic conditions[70], which agrees with the conclusion

drawn from section 2.3.1 that the flow cell detector does not add significant band spreading to the chromatograph.

Both the anode and cathode give usable signals, but the background current and the noise on the downstream cathode are much lower than the upstream anode. The background current is principally faradic current arising from the oxidation (or reduction) of electroactive impurities in

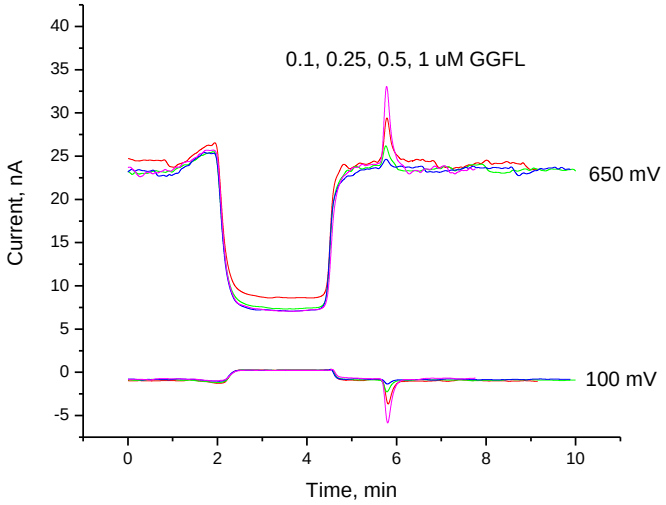

Figure 5 The chromatograms of GGFL

Mobile phase flow rate, 1 μL/min; Biuret reagent flow rate, 0.3 μL/min

the mobile phase and post-column reagent. Because the potential on the anode has to be set at a relative high value for Cu(II)-peptide to be oxidized, more species in the system are electroactive, thus creating higher background current. Noise is the random or periodic pattern superimposed on the steady-state background signal[71], representing the summation of spurious contributions from pump pulsation, flow cell hydrodynamics, static electricity, electronic amplification and etc. High background currents increase the susceptibility of the system to noise. The potential on the downstream cathode can be adjusted to give minimum background current, thus low noise.

Figure 6 demonstrates the linearity of the detection using peak heights. The regression analysis shows great linearity on both electrodes with R^2 value of 0.99885 on anode and 0.99958 on cathode. The detection limit is 10 nM, which is the concentration required to give a signal-to-noise ratio of 3.

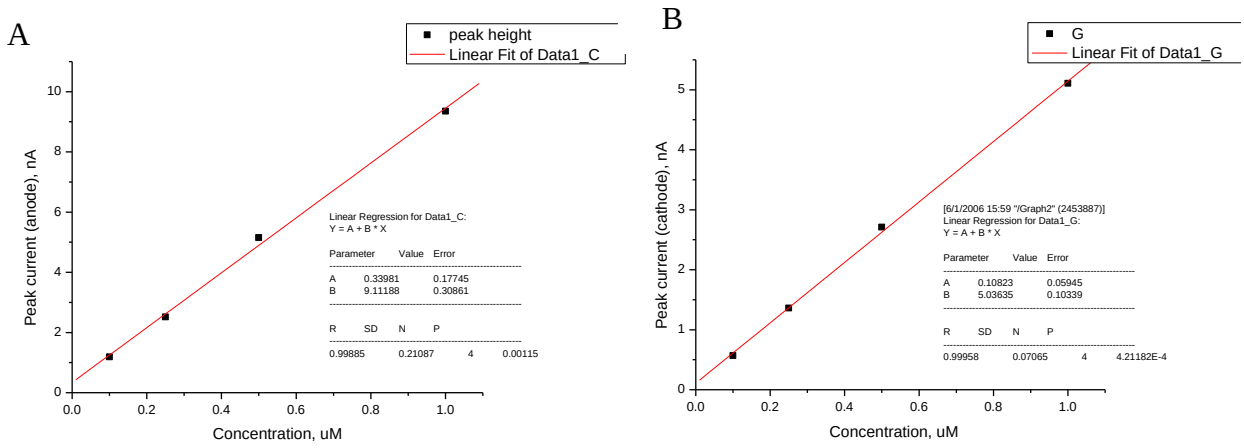

Figure 6 Working curves showing the linearity of detection on (A) anode and (B) cathode

2.3.2.2 Mixture of Enkephalin standards

The validation of capillary HPLC separation of enkephalins can be demonstrated with a mixture of enkephalin standards, YGGFL, YGGFM, and GGFL, GGFM, the hydrolysis products (Figure 7). The current responses of YGGFL and YGGFM on the anode are higher than their hydrolysis products with the same concentration, while lower on the cathode. Y (Tyr) is an electroactive amino acid, so peptides with Y are detectable without derivatization, however, the reaction with Cu (II) leads to increases in sensitivity for Y- containing peptides because the anode signal is actually the sum of the electroactive amino acid signal and the Cu (II) signal with appropriate potential applied[72]. This explains that YGGFL and YGGFM give higher current response on anode compared to their hydrolysis products with the same concentration. On the contrary, the cathode signals of Y-containing peptides are lower than their hydrolysis products. There are two

reasons for that. First, at the relatively long time scales of the mass transport process from the anode to the cathode in the dual electrode detection, tyrosine oxidations are chemically irreversible. Thus, the only carrier of signal for the cathode is Cu (III). Second, the oxidized product of the Y-containing peptide created on the anode, Y_{ox}-Cu(III)-peptide, can undergo chemical reaction to produce $Y_{ox'}$-Cu(III)-peptide. This process may be followed by further homogeneous intramolecular electron-transfer reaction, $Y_{OX'} - Cu(III) - peptide \rightarrow Y_{OX,OX} - Cu(II) - peptide$. Because the tyrosine oxidation product $Y_{ox,ox}$-Cu(II)-peptide cannot be reversibly reduced, the net current response on the cathode is depressed.

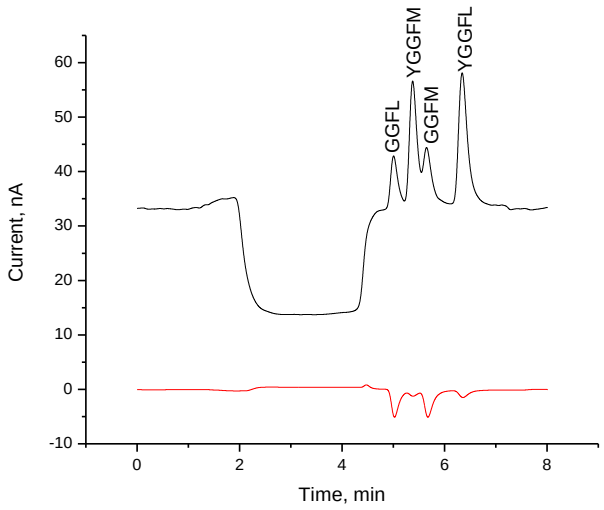

Figure 7 The chromatograph of 1 μM enkephalin standard

Conditions are the same as those in Fig. 5

2.3.3 Application of the dual electrode flow cell in rat brain sample extract analysis

Dual-electrode detection has better selectivity than single electrode detection in that the potential on the two electrodes can be set at different values for different detection purposes. In a parallel dual electrode configuration, a higher potential can be applied on one electrode so that the hard to oxidize (reduce) components can be detected. But at the same time, the chromatogram will be too complicated and the response from one or more desired components can often be obscured by interferences. The dilemma can be solved by setting the second electrode at a lower potential so that only the more easily oxidized (reduced) components will be detected with great selectivity. The low potential chromatogram usually features better detection limits because of decreased complexity of the chromatogram[73]. In a series dual electrode configuration, the products from the upstream detector can be detected at the downstream detector (oxidative-reductive detection). So those chemically or electrochemically irreversible species are not detected at the downstream electrode, which results in simple chromatograms on the downstream detector and easier peak identification[74].

Our peptide detection scheme is based on the biuret reaction of Cu(II) with peptides and uses a series dual electrode detector. The Cu(II)-peptide/Cu(III)-peptide electrochemistry is reversible with a half-wave potential around 0.5 V vs. Ag/AgCl: the Cu(II)-peptide is oxidized at the upstream anode, followed by reduction of Cu(III) back to Cu(II) at a downstream cathode. The potential on the downstream electrode can be set at a low reductive value, so that fewer species are electroactive and the irreversible electrochemical oxidation processes happening on the upstream electrode are eliminated. This is especially beneficial in selective peptide detection in biological samples, because biological samples usually have a complicated matrix of different electroactive components at high potentials.

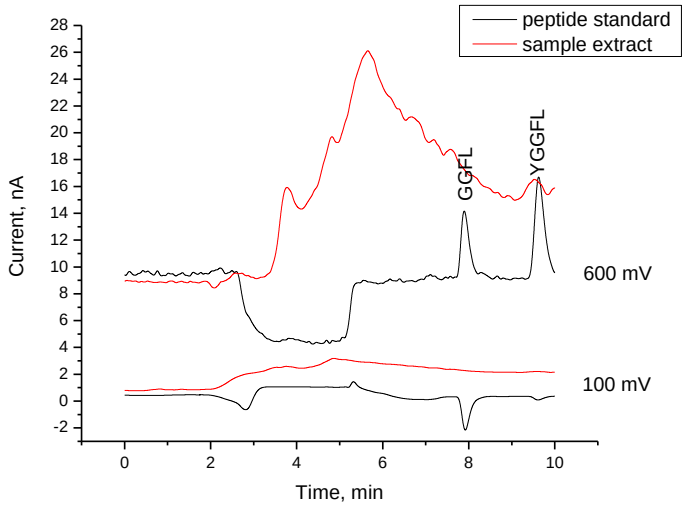

Figure 8 The chromatograms of rat brain slice extracts compared with peptide standard

Figure 8 shows the chromatographic analysis of rat brain slice extracts. Although the background current on the cathode is much lower than anode, not much information can be obtained from the chromatograms. The possible reason is that the column is over loaded and the sample is not well separated, which indicates that sample dilution is needed.

Because quantitative analysis of the rat brain sample is not necessary in this part of the work, sample dilution is done just to avoid column overloading and keep analyte concentration at a detectable range. Referring to the previous work done in our lab[75], the sample was diluted about 10 folds and spiked with GGFL peptide. The resulting chromatogram (Figure 9) on the upstream anode has very many peaks, in which case it is hard to identify the GGFL peptide signal. However, the chromatogram on the downstream cathode provides a much lower background and noise, which makes GGFL identification straightforward.

Although dilution of the sample helps to generate useful information, there is problem in the chromatograph reproducibility. A shift in retention time (~1 minute) was noticed after repeated sample injection. The retention time shift was attributed to change in the flow rate.

Flow rate through the column is controlled by the column back pressure, which will increase when there is irreversible sample adsorption to the column. This results in lower flow rate and thus longer retention time for analytes.

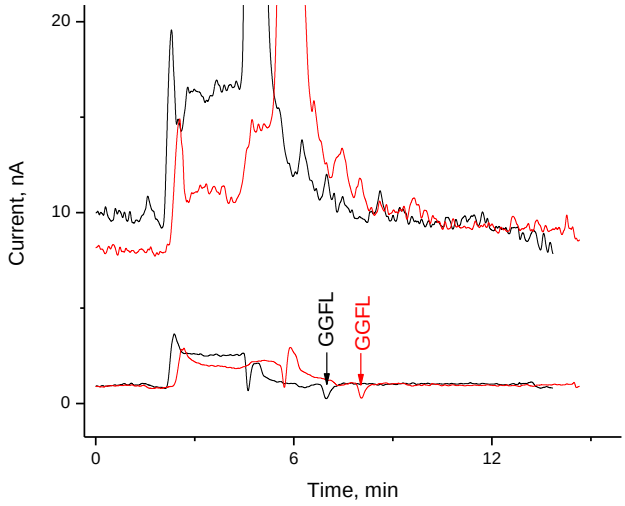

Figure 9 The chromatograms of diluted rat brain slices extract sample spiked with GGFL, the red trace shows the second injection

The problem can be solved if the irreversibly adsorbed sample components could be removed. Flushing the column with pure acetonitrile did not help restoring retention times. So we need to remove those irreversibly absorbed sample components before they are eluted to the column. It can be realized by using a guard column, a precolumn protection. However, the flow split prohibited an online precolumn from being implemented[75]. So we use an offline sample pretreatment for this purpose. The ZipTip is a pipette tip containing a small amount of reversed phase packing material, which can be regarded as a small offline guard column. By ZipTip treatment, those irreversibly adsorbed sample components will remain in the tip. Based on these concerns, the sample was treated with ZipTip according to the manufacture specifications and spiked with GGFL and YGGFL. The chromatograms (Figure 10) show great reproducibility. The

chromatograms are also much “cleaner” compared to Figure 9, which implies that some species might not be recovered by ZipTip.

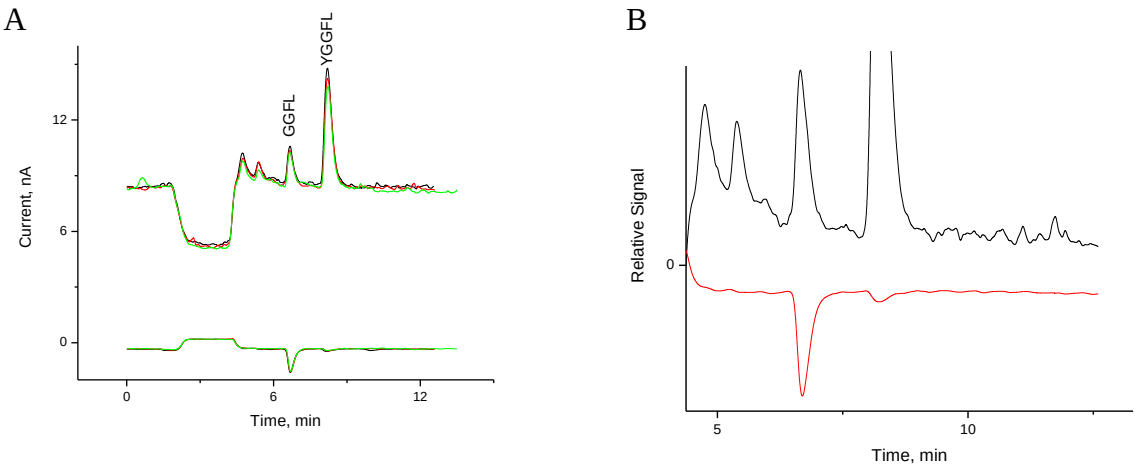

Figure 10 The chromatograms of diluted rat brain slice extract samples treated with ZipTip (A) three identical sample separation traces; (B) magnification of one chromatogram trace.

2.3.4 Optimization of the dual electrode flow cell and some theoretical considerations

As mentioned before, we worked on adapting a commercial detector, thin-layer flow cell from BAS, to the capillary format. The commercial thin-layer cell (Figure 11) consists of the following parts: the auxiliary electrode piece, a glassy carbon working electrode, a gasket and a reference electrode.

The auxiliary electrode piece includes inlet and outlet and a hole in the middle connecting to the reference electrode compartment. The inlet and outlet connections are made for 1/16" OD tubing used in traditional chromatography. To connect the cell to a capillary, we used Teflon tubing sleeves with 395µm (.015 IN) ID x 1/16” OD from Upchurch Scientific (Oak Harbor, WA) together with the PEEK fittings for 1/16" OD tubing. With the tubing sleeves, the cell can be

connected to the fused silica capillaries (365 μm OD) without significant dead volume. The BAS gasket channel is too wide, which can contribute to the cell-dead-volume. So we made our own gaskets using Teflon film from Dilectrix (Farmingdale, NY), which has a wide range of different film thickness to choose from. The channel is cut to be in a rectangular slit shape, 1 mm wide and 1 cm long. The edge of the channel should be smooth without any burr.

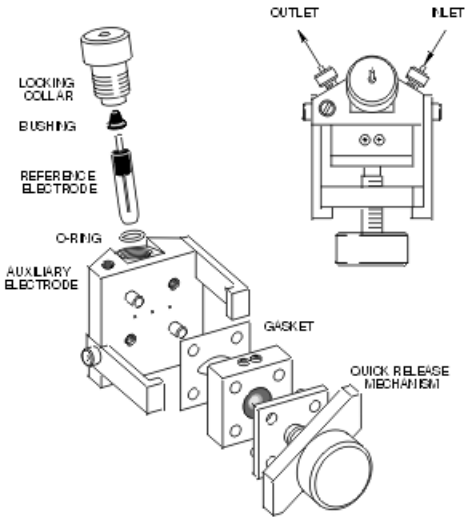

Figure 11 Diagram of a BAS thin-layer flow cell

Reprinted from http://www.bioanalytical.com/products/lc/flowcells.html with permission.

The electrode area affects the signal to noise ratio, thus the detector performance[76]. The diameter 3 mm dual glassy carbon electrode from BAS is not satisfactory when flow rate is in the microliter per minute range. And it does not fit with the 1 mm wide gasket channel. So we designed and made a diameter 1 mm dual glassy carbon electrode with two electrodes 0.5 mm apart.

Because the gasket defines the flow channel in the cell, the thickness of the gasket will affect the cell performance. We made the gaskets with the same channel shape using Teflon film with different thickness. Figure 12 shows the chromatograph of the same analyte GGFL under

the same chromatograph conditions except that the cell gasket has different thickness. There is no detectable current response with 6 µm thick gasket. The possible explanation is that the cell cannot be properly aligned with this extremely thin gasket, which might cause leakage in the cell.

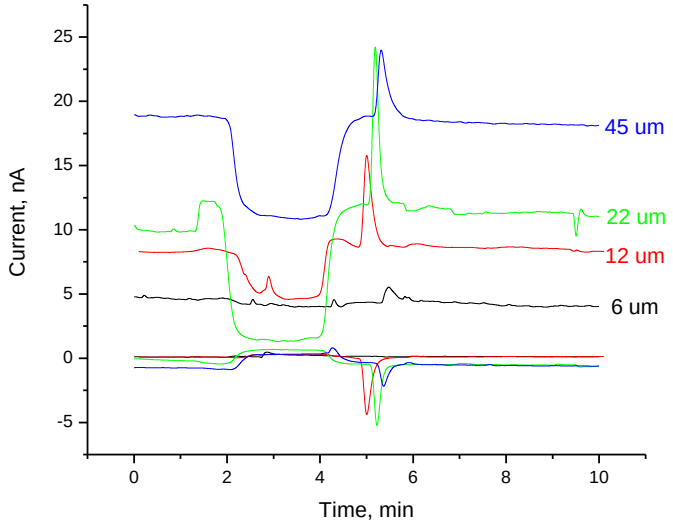

Figure 12 The chromatograms of 1 µM GGFL with different gasket thickness

Conditions are the same as those in Fig. 5

The detailed flow cell detector performance with different gasket thickness is shown in Table 1.

GGFL retention time increases with increasing gasket thickness. Given the same volume flow rate, the linear velocity of the flow crossing through is lower when the gasket is thicker. So it takes longer time for the analyte to get to the electrode when the gasket is thicker.

The peak current on the upstream anode shows dependence on the gasket thickness. The potential on the upstream electrode is set at a "mass-transfer limited" value, so the current depends on the electroactive species mass transfer. There are two components for mass transfer process in a stationary system, migration and diffusion. Migration can be ignored and diffusion is dominant provided having enough supporting electrolyte in the system. In the flow cell system,

there is another mass transfer factor besides diffusion: bulk fluid motion, which also carries analyte from the bulk of solution to a point near the electrode. Equations relating the steady-state current and solution velocity have been theoretically derived[77-79]. Most research work showed that the current output is dependent on the cube root of the linear velocity across the electrode surface. But this relationship is valid only when the coulometric yield of the cell is less than 10%[80]. With the low flow rate involved in capillary LC system, higher values of coulometric yield are often encountered and a more complex behavior is then observed[81]. There is another possibility that the two diffusion layer of working and auxiliary electrodes may overlap and become "coupled"[82] when the gasket is sufficiently thin. So it is possible that the oxidative product on the working electrode may be reduced on the auxiliary electrode and diffused back to the working electrode. Based on the discussion, the current response should decrease with increasing gasket thickness, which explains why the current response with 45 μm gasket is lower than that of 22 μm cell. The fact that we observed smaller current response with 12 μm gasket than 22 μm gasket might be due to possible leakage with very thin gasket.

The collection efficiency decreases with increasing gasket thickness. The collection efficiency is calculated as the ratio of the cathode peak current to the anode peak current, which stands for the fraction of upstream products that are converted at the downstream detector. With thicker gasket, larger fraction of the species produced on the upstream electrode will diffuse away before they get to the downstream electrode, as the linear velocity is lower.

Table 1 Influence of the gasket thickness on the cell performance

Gasket thickness (μm)	Retention time (min)	Anode peak current (nA)	Anode peak area (nC)	Cathode peak current(nA)	Cathode peak area (nC)	Sensitivity on anode (nC/pmol)	Collection efficiency
12	5.00	7.1	87	4.4	50	51	0.57
22	5.16	9.4	116	4.6	52	67	0.45
45	5.29	6.1	75	1.8	21	42	0.28

3.0 MODIFICATION OF A GOLD ELECTRODE FOR BIURET-BASED PEPTIDE AMPEROMETRIC DETECTION

3.1 INTRODUCTION

Our attempt to miniaturize the separation and detection system will lead us to the "lab-on-a-chip" field, so we need to consider both the chemistry and the technical feasibility in choosing electrode material. Carbon is widely used for electroanalytical purposes, due to its low cost, minimal fouling and wide useful potential range especially in the positive direction[83]. Carbon electrodes used in a microchip are usually in the forms of carbon fiber, carbon paste or carbon ink[84]. However, screen-printed carbon ink electrodes and carbon paste electrodes are not compatible with organic solvents, and carbon fibers are generally not rugged[85]. Metal electrodes, including gold, platinum, copper and palladium, are commonly used for microchip EC due to the relative ease with which they can be evaporated or sputtered[86]. One drawback to the use of metal electrodes is their tendency to become fouled when they are used for the detection of peptides, amino acid and biological samples. Chemically modifying the electrodes can change the surface properties of the metal electrodes. It is well known that gold can form covalent bond with thiols by self-assembly[87]. This method is advantageous: the process is simple which only involves immersing the electrode into a dilute thiol solution; the self-assembled monolayer is stable and can be easily removed when needed.

In the biuret-based peptide detection scheme, Cu(II)-peptide is oxidized to Cu(III)-peptide above 0.5 V vs. Ag/AgCl in pH 10 buffer. Gold gives high oxidative background current in that potential range, which makes quantitative peptide detection very difficult. Thus, there are some requirements in choosing appropriate thiol molecules to modify Au: 1) it should block gold surface from water so that suppress background current; 2) electron transfer can still happen through the layer; 3) the modification material should be inert and stable in the media (mobile phase and biuret reagent). Alkanethiol, which is often used in gold modification, is not desirable because electron transfer can only happen through tunneling which is not sensitive enough for detection purpose. Aromatic thiol with extended and closed aromatic system, on the other hand, is possible in that electron transfer can occur through delocalized π bond. Based on these concerns, aromatic thiol compounds seem to be a good candidate.

This part of the work will focus on two commercially available aromatic thiols, 4, 4'-dithiodipyridine and 2-naphthalenethiol. 4, 4'-Dithiodipyridine (PySSPy) will form 4-mercaptopyridine (PyS) monolayer on gold surface in self assembly process[88].

3.2 EXPERIMENTAL

3.2.1 Reagents

Reagents and sources were as follows: 2-naphthalenethiol, 4, 4'-dithiodipyridine, ACS grade sodium carbonate and sodium bicarbonate, Sigma-Aldrich; disodium tartrate dihydrate and copper sulfate pentahydrate, J. T. Baker (Phillipsburgh, NJ); des-tyr leu enkephalin (GGFL), BACHEM (King of Prussia, PA).

The copper sulfate pentahydrate was recrystallized from water. The disodium tartrate dihydrate was recrystallized from dilute NaOH. All other reagents were used without further purification.

All solutions were made with Milli-Q (Millipore, Billerica, MA) house-deionized water.

3.2.2 Electrode pretreatment and thiol adsorption

Immediately before use, the electrode was polished successively with 1, 0.3 and 0.05 μm Buehler (Lake Bluff, IL) alumina in aqueous slurries, and ultrasonicated in Millipore water to remove alumina particles. Then it was rinsed thoroughly with Millipore water and ethanol before thiol modification.

The thiol monolayer was prepared by keeping the gold electrode in 10 mM 2-naphthalenethiol or 4, 4'-dithiodipyridine ethanol solution for 1 hour. After the adsorption of thiol, the electrode was rinsed with ethanol, then Millipore water.

Electrode surface cleaning before modification is crucial to the modification layer quality. Also, modification conditions, e.g. the solvent used to dissolve the modification molecules and the immersion time, are important for the result. For example, short immersion times result in still too many defects which allow easy water access to the surface and local oxide growth.

3.2.3 Cyclic voltammetry

Gold working electrode of 2 mm diameter (CH Instruments, Inc.) was used as the substrate for thiol modification test and CV characterization. The glassy carbon electrode used as comparison was homemade. It was constructed by sealing glassy carbon (Sigradur) of 1 mm diameter in

glass with Torr Seal (Varian Vacuum Technologies). A platinum coil of large surface area was used as the counter electrode, and An Ag/AgCl, 3 M NaCl (BAS, Model RE-5B) reference electrode was used and all the potentials were referred to it. The barrier property of the monolayer was studied using pH 10 buffer solution (0.24 M $NaHCO_3$ / Na_2CO_3). The Cu-peptide solution was prepared by adding peptide to the biuret reagent (0.24 M $NaHCO_3$, 0.24 M Na_2CO_3, 12.0 mM Na_2Tar and 2.0 mM $CuSO_4$) with the final concentration of 10 μM Cu-GGFL.

Cyclic voltammetry was also done on the cathode(downstream) electrode in a dual-electrode flow cell, while the potential on the anode(upstream) electrode was kept at an oxidative potential (600 mV vs. Ag/AgCl). The instrumentation set-up was the same as that in Chapter 2. The solution pumped through the flow cell was 50 μM Cu(II)-GGFL in the biuret reagent. The dual gold working electrode piece of 3 mm diameter from BAS was used as working electrode.

Cyclic voltammetry was carried out with a BAS Epsilon EC potentiostat with Epsilon EC software. The electrochemical equipment was housed in a faradaic cage to reduce electronic noise. The potential ranges and scan rates used are shown in the respective diagrams.

3.2.4 Capillary liquid chromatography

The instrumentation set-up was the same with that in Chapter 2, except that the working electrode here was the dual gold working electrode piece of 3 mm diameter from BAS.

3.3 RESULTS AND DISCUSSION

3.3.1 Electrochemistry

3.3.1.1 2-Naphthalenethiol

Cyclic voltammetry is used for electrochemical characterization of 2-naphthalenethiol modified gold electrode. Figure 13 shows the cyclic voltammograms of a bare gold electrode and a 2-naphthalenthiol modified gold electrode in a pH 10 carbonate buffer solution and Cu(II)-GGFL solution.

At a bare gold electrode (Figure 13A), anodic current arises at potential positive than 0.5 V vs. Ag/AgCl in a pH 10 buffer solution, followed by the corresponding cathodic peak at approximately 0.3 V. This results from the surface process of gold oxidation and reduction. Cu(II)-GGFL in the same buffer gives an ill-defined cyclic voltammogram. One explanation is that the gold surface properties will change when the applied potential is above the gold oxidation onset value. So the Cu(II)-GGFL/Cu(III)-GGFL redox is not happening on a metallic gold, but some form of gold oxide. The current response is also the combination of the aqueous electroactive species oxidation/reduction process and the Au oxide formation/removal.

Modification of Au electrode with 2-naphthalenthiol suppresses anodic current from gold surface oxide formation and thus the stripping peak from the surface oxide reduction (Figure 13B). It indicates that 2-naphthalenethiol forms a barrier-type film which prevents the formation of anodic oxide on a gold electrode. Ideally, the monolayer is well-ordered and dense enough so that water cannot penetrate to the Au surface where its presence is required for oxide growth. This is similar to the behavior of self-assembled monolayer (SAM) of alkanethiol on gold surface[58, 89-95]. The cyclic voltammogram of the redox couple, Cu(II)-GGFL/Cu(III)-GGFL,

shows well-defined redox peaks. There are two oxidative peaks in the voltammograms. This is in agreement with the rotating ring-disk electrode study[69] that there are two generic forms of the complexes, Cu(II)-NNNN and Cu(II)-NNNO, with respective $E_{1/2}$ values of 0.45 V and 0.7 V vs. Ag/AgCl.

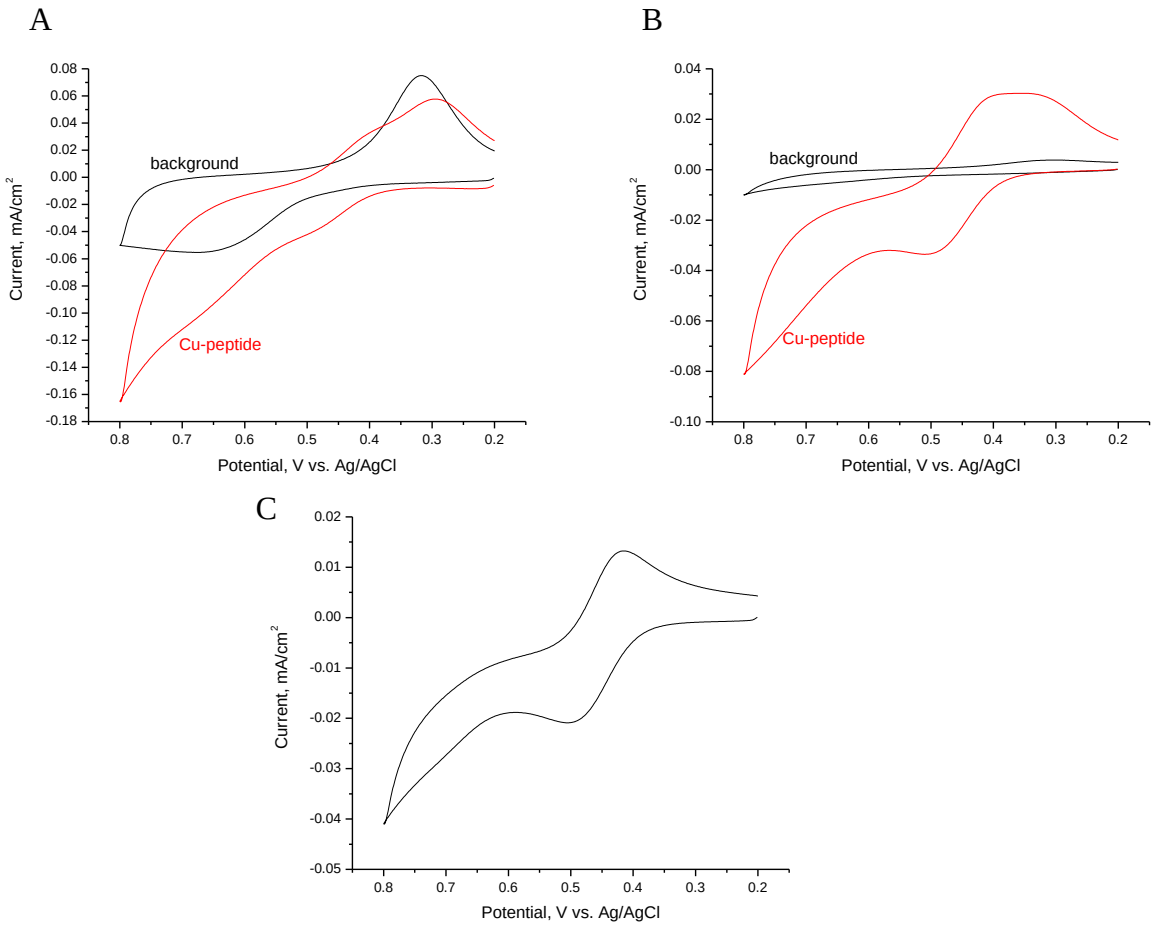

Figure 13 Cyclic voltammograms of different electrode surfaces in buffer and Cu-peptide solution (pH 10.4 carbonate buffer and 10 μM Cu-GGFL biuret solution)

The peak potential, peak shape and separation are similar to those on a glassy carbon (Figure 13C). However, the current density of the modified Au is higher than that of a glassy carbon under the same conditions. Previous research work on alkanethiol SAM shows that the integrity of the monolayer is seldom perfect[58, 90, 95]. Pinholes are usually present in the monolayer, so both the electrolyte and redox couple have access to the gold substrate at the pinholes. The behavior exhibited by the alkanethiol modified electrode with pinholes resembles a microarray electrode[96-98]. The proposed reason why the current density of 2-naphthalenethiol modified Au is higher than that of a glassy carbon is that the current response in this case is a sum of the pinhole microelectrode effect and the electron transfer through the monolayer. The electron transfer through the monolayer is much more effective than that through alkanethiol SAMs, because the tunneling process is highly facilitated through the delocalized π-electrons[99].

3.3.1.2 4, 4'-dithiodipyridine

It is known that 4, 4'-dithiodipyridine (PySSPy) can form 4-mercaptopyridine (PyS) monolayer on Au, which has been used to immobilize proteins for direct electrochemistry study[88, 100-102]. CV result (Figure 14) shows that Au oxide formation is not completely hindered on the PyS modified gold surface. In this case, it is hard to quantify the current response generated from the electroactive species in the electrolyte.

Obviously pyridinethiol monolayer features more defects and is less dense compared to naphthalenethiol. In the case of well studied alkanethiol SAMs, it is known that the chain length has a significant effect on the structural properties of the monolayer: longer-chain alkanethiols form ordered films on gold because of increased van der Waals interactions between chains, and shorter-chain alkanethiols are generally more disordered[94, 103]. This can be one of the reasons why PyS monolayer quality is poorer than naphthalenethiol monolayer. Another possible reason is that PyS modified surface showed more hydrophilicity than the 2-naphthalenethiol modified surface due to the pyridine ring.

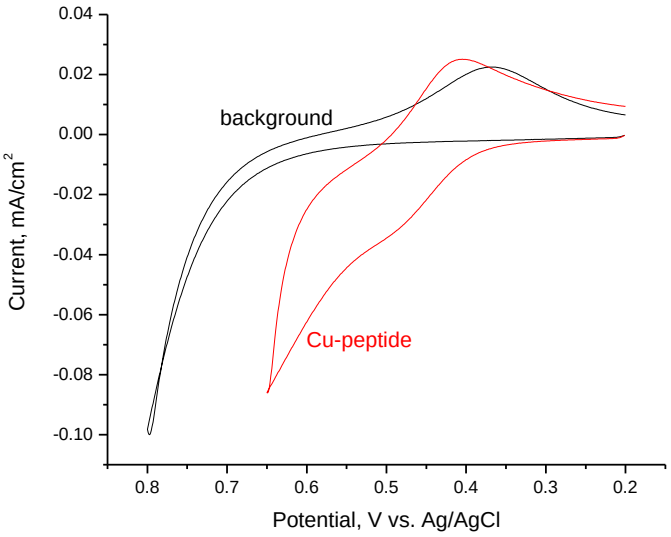

Figure 14 Cyclic voltammograms of a pyridine thiol modified Au in (a) pH 10.4 carbonate buffer and (b) 10 μM Cu-GGFL biuret solution

CV results show that 2-naphthalenethiol is a better choice than PyS. The following discussions are based on experiments done with 2-naphthalenethiol monolayer. It is expected that aromatic thiol with larger conjugated π system should form more ordered monolayer and have better conductivity because of decreasing band-gap (or HOMO-LUMO separation)[104]. But

at the same time, the solubility decreases and synthetic routes become increasingly more difficult. Thus, anthracenethiol seems to be a promising molecule and its synthesis is relatively easy, so will be part of our future work.

3.3.1.3 CVs of the modified Au electrode in a flow cell

Based on the CV results, the potential on the upstream anode in the dual-electrode flow cell detector can be set above 0.55 V vs. Ag/AgCl to oxidize Cu (II)-peptide. To get the optimal

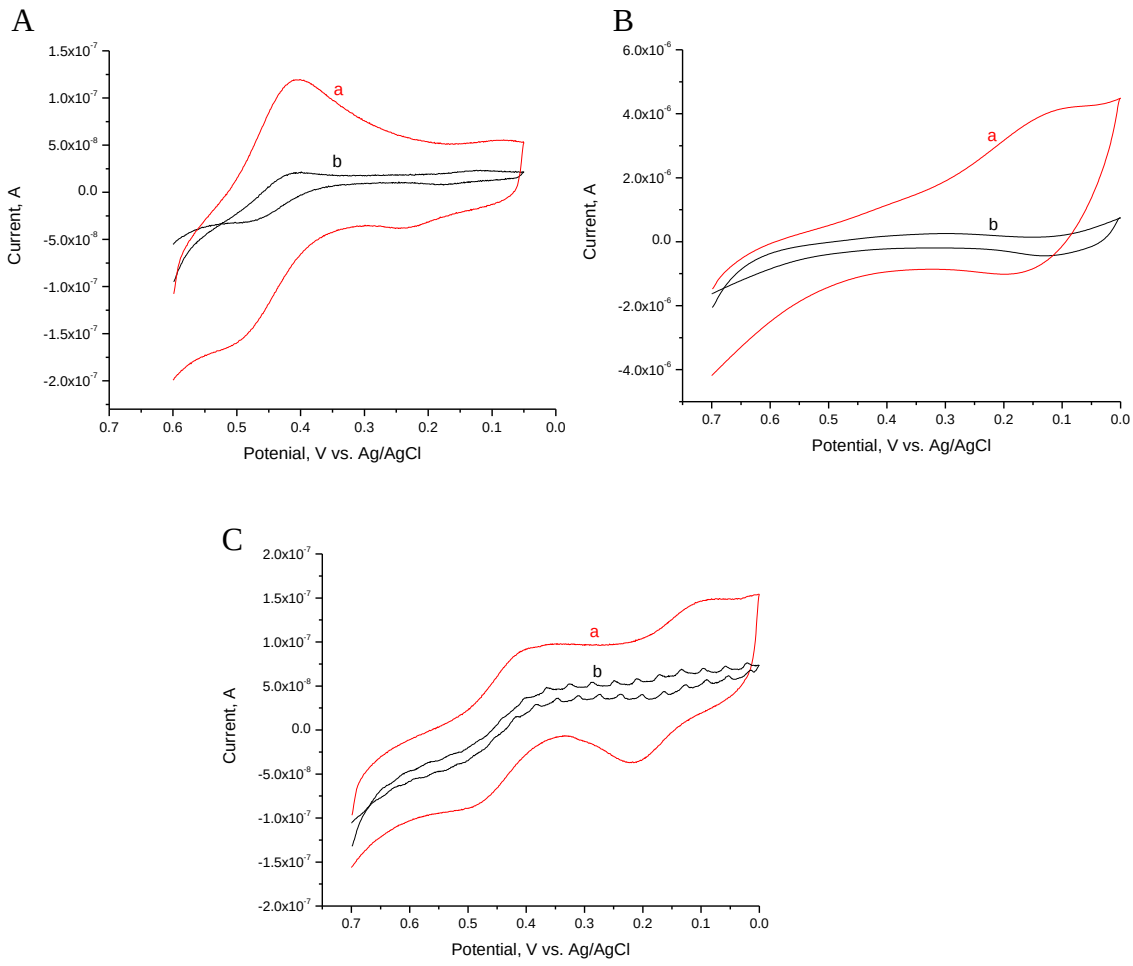

Figure 15 Cyclic voltammograms of the cathode in the flow cell at different scan rates (a 200 mV/s, b 20 mV/s) with potential on the anode kept at 700 mV vs. Ag/AgCl

detection potential on the downstream cathode, CV is carried out on the downstream electrode with flow cell setup. The potential on the anode is held at positive value (> 0.5 V vs. Ag/AgCl) while scanning the potential on the cathode from positive to negative (Figure 15A). There is a reductive peak at ~0.4 V vs. Ag/AgCl, which is expected to be the reduction of Cu(III)-peptide. When the potential goes more negative, another reductive current peak appears at ~0.15 V, which can be attributed to Cu(II)-peptide/Cu(I)-peptide reduction. The standard $E_{1/2}$ for Cu^{2+}/Cu^{+} is 0.153 V vs. NHE[105], which equals -0.056 V vs. Ag/AgCl. However, by the presence of ligand, peptide in this case, the reduction potential of Cu^{2+} shifts. It was found that the Cu(II) is reduced to Cu(I) at 0.096 V vs. Ag/AgCl in the presence of Ac-PHGGGWGQ-NH_2, a unit of the octarepeat peptide of the prion protein[106].

The results are similar to those on a glassy carbon electrode (Figure 15C). On the contrary, no apparent reduction peak can be seen on a bare Au electrode (Figure 15B).

3.3.2 Capillary liquid chromatography

Results in the previous section give the criteria for choosing appropriate potentials for peptide detection after capillary liquid chromatography separation. Figure 16 shows the simple chromatograph of GGFL detected using bare Au and 2-naphthalenethiol modified Au. A bare gold electrode gives very high background current and the signal is very low. 2-naphtalenthiol modified Au shows good detection trace and the signal current is comparable to those done with a glassy carbon (Figure 5).

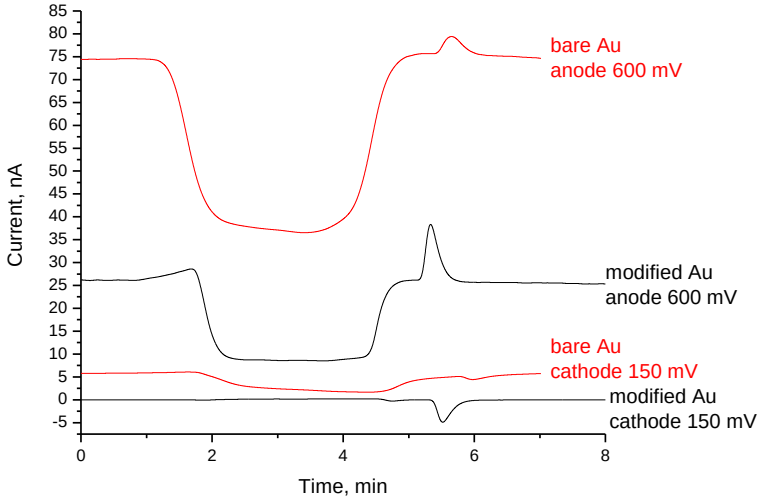

Figure 16 Chromatograms of 1 µM GGFL with bare Au and 2-naphthalenethiol modified Au

3.3.3 Stability of 2-naphthalenethiol modification monolayer

The chromatogram shows that 2-naphthalenethiol modified Au works well in biuret based peptide detection. However, stability of the modified electrode needs to be tested before it can be used in routine detection work. The stability test is done by repeating sample injection and recording the current response over time. The potential was on with flow running through the cell during the period. The current decreases about 5% over 3 hours (Figure 17), which shows pretty good stability of the modification layer. However, the current decays exponentially over days with flow running through the flow cell, but the potential was off between days (Figure 18). Current difference between 2nd day and 3rd day after modification shows that current decays faster when the potential is on.

The possible reason is that structure of the modification layer changes over time, becoming less ordered or even desorbed from the Au surface. The modified electrode is exposed to the biuret reagent/mobile phase flow, which is basic with pH value of 10. It is known that

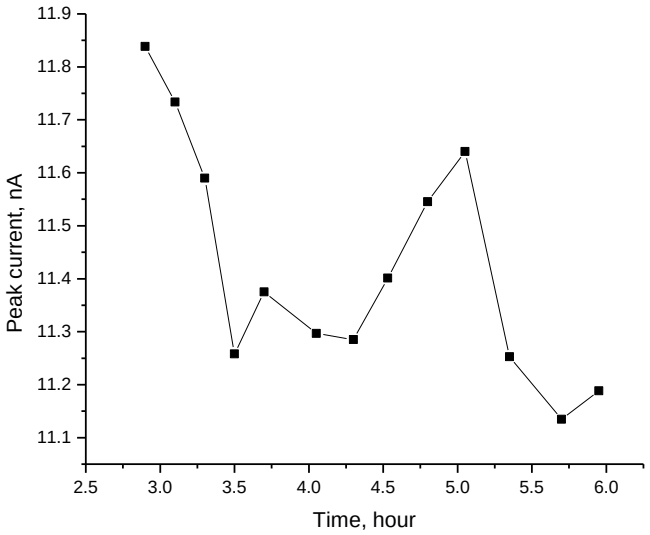

Figure 17 Current response of repeated GGFL injection on modified Au electrode over hours

alkanethiol head group is electrochemically oxidizable or reducible in strong base[107, 108]. The reductive desorption, $AuSR + 1e^- \rightarrow Au(0) + RS^-$, has a half wave potential of -0.9 V vs. Ag/AgCl in 0.5 M KOH. The oxidative desorption is related to the reaction $AuSR + 2H_2O \rightarrow Au(0) + RSO_2^- + 3e^- + 4H^+$, which has a half wave potential of 0.9 V vs. Ag/AgCl in a pH 10 buffer. So it is possible that the naphthalenethiol desorbs from the gold surface in the basic buffer over time. But as long as the applied detection potential is not extremely positive or negative, the desorption process is fairly slow. Based on the experimental results, the modification monolayer can last for hours without significant sensitivity loss. If needed, the modification monolayer can be easily removed by electrochemical desorption. Then the simple self assembly process can be carried out again to create a flesh modification monolayer.

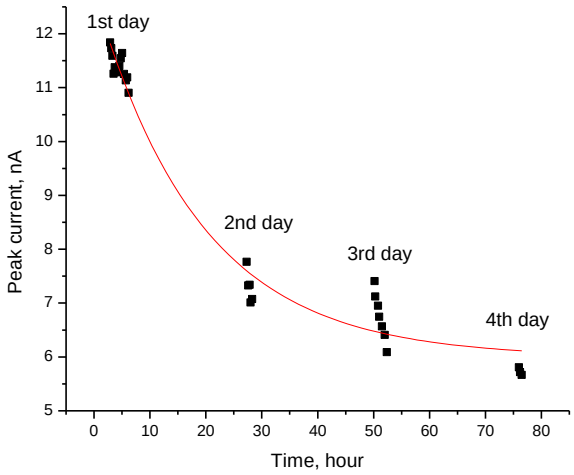

Figure 18 Current response of repeated GGFL injection on modified Au electrode over days

BIBLIOGRAPHY

(1) Aguilar *HPLC of peptides and proteins: methods and protocols*; Humana Press: Totowa, New Jersey, 2004.
(2) Mant, C. T. H., R. S. *Analysis of peptides by high performance liquid chromatography*; CRC Press: Boca Raton, 1996.
(3) Shen, H. L., M. W.; Kennedy, R. T. *Journal of Chromatography, B: Biomedical Sciences and Applications* **1997**, *704*, 43-52.
(4) Vissers, J. P. C., H. A.; Cramers, C. A. *Journal of Chromatography, A* **1997**, *779*, 1-28.
(5) Jinno, L. *Chromatographia* **1988**, *25*, 1004-1011.
(6) Novotny, M. *Analytical Chemistry* **1988**, *60*, 502A-510A.
(7) Saito, Y. J., K.; Greibrokk, T. *Journal of Separation Science* **2004**, *27*, 1379-1390.
(8) Regnier, F. E.; He, B.; Lin, S.; Busse, J. *Trends in Biotechnology* **1999**, *17*, 101-106.
(9) Effenhauser, C. S. *Topics in Current Chemistry* **1998**, *194*, 51-82.
(10) McEnery, M.; Tan, A.; Glennon, J. D.; Alderman, J.; Patterson, J.; O'Mathuna, S. C. *Analyst (Cambridge, United Kingdom)* **2000**, *125*, 25-27.
(11) Uchiyama, K. N., H.; Hobo, T. *Analytical Bioanalytical Chemistry* **2004**, *379*, 375-382.
(12) Kamahori, M. W., Y.; Muri, J.; Taki, M.; Miyagi, H *Journal of Chromatography* **1989**, *465*, 227-232.
(13) Kientz, C. V., A. *Journal of high resolution chromatography* **1988**, *11*, 294-296.
(14) Vindevogel, J. S., G.; Dewaele, C.; Verzele, M. *Journal of high resolution chromatography* **1988**, *11*.
(15) Bruin, G. J. M.; Stegeman, G.; Van Asten, A. C.; Xu, X.; Kraak, J. C.; Poppe, H. *Journal of Chromatography* **1991**, *559*, 163-181.
(16) Gluckman, J. C. N., M. *Journal of high resolution chromatography* **1985**, *8*, 672-677.
(17) Gluckman, J. C. S., D. C.; Novotny, M. *Analytical Chemistry* **1985**, *57*, 1546-1552.
(18) Xue, A. D., M.; Foret, F.; Karger B. L. *Rapid Commun Mass Spectrom* **1997**, *11*, 1253-1256.
(19) Lazar, I. M. R., R. S.; Sundberg, S.; Ramsey, J. M. *Analytical Chemistry* **1999**, *71*, 3627.
(20) Wang, J. *Talanta* **2002**, *56*, 223-231.
(21) Kilts, C. D. K., D. L.; Nemeroff, C. B. *Life Science* **1996**, *59*, 911.
(22) Bennett, G. W. B., M. P.; Marsden, C. A. *Life Science* **1981**, *29*, 1001.
(23) Reynolds, N. C. K., B. M.; Fleming, L. H. *Electroanalysis* **1995**, *7*, 1177.
(24) Koller, M. E., H. *Analytica chimica Acta* **1997**, *352*, 31.
(25) Allison, L. A. M., G. S.; Shoup, R. E. *Analytical Chemistry* **1984**, *56*, 1089.
(26) Nussbaum, M. A. P., J. E.; Staerk, D. U.; Lunte, S. M.; Riley, C. M. *Analytical Chemistry* **1992**, *64*, 1259.
(27) Chen, J.-G.; Weber, S. G. *Analytical Chemistry* **1995**, *67*, 3596-3604.

(28) Chen, J.-G.; Woltman, S. J.; Weber, S. G. *Journal of Chromatography, A* **1995**, *691*, 301-315.
(29) Lunte, S. M.; Martin, R. S.; Lunte, C. E. *Electroanalytical Methods for Biological Materials* **2002**, 461-490.
(30) Lin, B. L.; Colon, L. A.; Zare, R. N. *Journal of Chromatography, A* **1994**, *680*, 263-270.
(31) Zhong, M.; Zhou, J.; Lunte, S. M.; Zhao, G.; Giolando, D. M.; Kirchhoff, J. R. *Analytical Chemistry* **1996**, *68*, 203-207.
(32) Zhong, M.; Lunte, S. M. *Analytical Chemistry* **1999**, *71*, 251-255.
(33) Holland, L. A.; Lunte, S. M. *Analytical Chemistry* **1999**, *71*, 407-412.
(34) Holland, L. A.; Harmony, N. M.; Lunte, S. M. *Electroanalysis* **1999**, *11*, 327-330.
(35) Henry, C. S. *Microchip capillary electrophoresis: methods and protocols*; Humana Press: Totowa, 2006.
(36) Martin, R. S.; Gawron, A. J.; Lunte, S. M.; Henry, C. S. *Analytical Chemistry* **2000**, *72*, 3196-3202.
(37) Baldwin, R. P.; Roussel, T. J., Jr.; Crain, M. M.; Bathlagunda, V.; Jackson, D. J.; Gullapalli, J.; Conklin, J. A.; Pai, R.; Naber, J. F.; Walsh, K. M.; Keynton, R. S. *Analytical Chemistry* **2002**, *74*, 3690-3697.
(38) Hebert, N. E.; Kuhr, W. G.; Brazill, S. A. *Electrophoresis* **2002**, *23*, 3750-3759.
(39) Gawron, A. J.; Martin, R. S.; Lunte, S. M. *Electrophoresis* **2001**, *22*, 242-248.
(40) Martin, R. S.; Gawron, A. J.; Fogarty, B. A.; Regan, F. B.; Dempsey, E.; Lunte, S. M. *Analyst (Cambridge, United Kingdom)* **2001**, *126*, 277-280.
(41) Wu, C.-C.; Wu, R.-G.; Huang, J.-G.; Lin, Y.-C.; Chang, H.-C. *Analytical Chemistry* **2003**, *75*, 947-952.
(42) Yan, J.; Du, Y.; Liu, J.; Cao, W.; Sun, X.; Zhou, W.; Yang, X.; Wang, E. *Analytical Chemistry* **2003**, *75*, 5406-5412.
(43) Liu, Y.; Vickers, J. A.; Henry, C. S. *Analytical Chemistry* **2004**, *76*, 1513-1517.
(44) Ertl, P.; Emrich, C. A.; Singhal, P.; Mathies, R. A. *Analytical Chemistry* **2004**, *76*, 3749-3755.
(45) Garcia, C. D.; Henry, C. S. *Analytical Chemistry* **2003**, *75*, 4778-4783.
(46) Wilke, R.; Buttgenbach, S. *Biosensors & Bioelectronics* **2003**, *19*, 149-153.
(47) Wang, J.; Ibanez, A.; Prakash Chatrathi, M. *Journal of the American Chemical Society* **2003**, *125*, 8444-8445.
(48) Wang, J.; Chatrathi, M. P. *Analytical Chemistry* **2003**, *75*, 525-529.
(49) Pourbaix, M. *Atlas of electrochemical equilibria in aqueous solutions*; Pergamon: Oxford, 1966.
(50) Burke, L. D.; Nugent, P. F. *Gold Bulletin (London)* **1997**, *30*, 43-53.
(51) Burke, L. D.; Twomey, T. A. M. *Journal of Electroanalytical Chemistry and Interfacial Electrochemistry* **1984**, *167*, 285-290.
(52) Conway, B. E. *Progress in Surface Science* **1995**, *49*, 331-452.
(53) Creager, S. E.; Hockett, L. A.; Rowe, G. K. *Langmuir* **1992**, *8*, 854-861.
(54) Bertilsson, L.; Liedberg, B. *Langmuir* **1993**, *9*, 141-149.
(55) Burke, L. D.; Collins, J. A.; Horgan, M. A.; Hurley, L. M.; O'Mullane, A. P. *Electrochimica Acta* **2000**, *45*, 4127-4134.
(56) Carvalhal, R. F.; Freire, R. S.; Kubota, L. T. *Electroanalysis* **2005**, *17*, 1251-1259.
(57) Hoogvliet, J. C.; Dijksma, M.; Kamp, B.; Van Bennekom, W. P. *Analytical Chemistry* **2000**, *72*, 2016-2021.

(58) Ulman, A. *Introduction to ultrathin organic films, from Langmuir-Blodgett to self-assembly*; Academic Press, Inc.: New York, 1991.
(59) Wang, W.; Lee, T.; Reed, M. A. *Reports on Progress in Physics* **2005**, *68*, 523-544.
(60) Ulman, A.; Kang, J. F.; Shnidman, Y.; Liao, S.; Jordan, R.; Choi, G.-Y.; Zaccaro, J.; Myerson, A. S.; Rafailovich, M.; Sokolov, J.; Fleischer, C. *Reviews in Molecular Biotechnology* **2000**, *74*, 175-188.
(61) Boyd, B. W.; Kennedy, R. T. *Electroanalytical Methods for Biological Materials* **2002**, 491-521.
(62) Aoke, K. O., J. *Journal of Electroanalytical Chemistry and Interfacial Electrochemistry* **1981**, *122*, 19.
(63) Boldt, F.-M.; Baltes, N.; Borgwarth, K.; Heinze, J. *Surface Science* **2005**, *597*, 51-64.
(64) Hepel, T. P., W.; Osteryoung, J. *Journal of physical Chemistry* **1983**, *87*, 1278.
(65) Knox, J. H. G., M. T. *Journal of Chromatography* **1979**, *186*, 405.
(66) Beisler, A. T.; Schaefer, K. E.; Weber, S. G. *Journal of Chromatography, A* **2003**, *986*, 247-251.
(67) Sahlin, E.; Beisler, A. T.; Woltman, S. J.; Weber, S. G. *Analytical Chemistry* **2002**, *74*, 4566-4569.
(68) Pluskal, M. G. *Nature Biotechnology* **2000**, *18*, 104-105.
(69) Woltman, S. J.; Alward, M. R.; Weber, S. G. *Analytical Chemistry* **1995**, *67*, 541-551.
(70) Xu, H.; University of Pittsburgh, 2005, pp 56.
(71) Gratzl, M.; Pungor, E. *Zhurnal Analiticheskoi Khimii* **1988**, *43*, 541-554.
(72) Tsai, H.; Weber, S. G. *Analytical Chemistry* **1992**, *64*, 2897-2903.
(73) Lunte, C. E.; Kissinger, P. T. *Analytical Chemistry* **1983**, *55*, 1458-1462.
(74) Roston, D. A., Kissinger, P. T. *Analytical Chemistry* **1982**, *54*, 429-434.
(75) Beisler Amy, T., University of Pittsburgh, Pittsburgh, 2003.
(76) Long, J. T. W., Stephen G. *Analytical Chemistry* **1988**, *60*, 2309-2311.
(77) Roosendaal, E. M. M. P., H. *Analytica Chimica Acta* **1984**, *158*, 323.
(78) Weber Stephen, G. P., W. C. *Analytica Chimica Acta* **1978**, *100*, 531.
(79) Meyer, R. E. B., M. C.; Lantz, P. M.; Posey, F. A. *Journal of Electroanalytical Chemistry* **1971**, *30*, 345.
(80) Weber Stephen, G. *Journal of Electroanalytical Chemistry* **1983**, *145*, 1.
(81) Carlsson, A. L., K. *Journal of Chromatography* **1985**, *350*, 169-178.
(82) Paddon, C. A. P., Gareth J.; Thiemann, Thies; Marken, Frank *Electrochemistry Communications* **2002**, *4*, 825-831.
(83) McCreery, R. L., Cline, K. K., *Laboratory Techniques in Electroanalytical Chemistry*; Marcel Dekker: New York, 1996.
(84) Scott, M. R. *Microchip Capillary Electrophoresis, Methods and Protocols*; Humana Press: Totowa, New Jersey, 2006.
(85) Lacher, N. A.; Garrison, K. E.; Martin, R. S.; Lunte, S. M. *Electrophoresis* **2001**, *22*, 2526-2536.
(86) Fischer, D. J.; Vandaveer, W. R. I. V.; Grigsby, R. J.; Lunte, S. M. *Electroanalysis* **2005**, *17*, 1153-1159.
(87) Dubois, L. H. M., R. G. *Anal. Rev. Phys. Chem.* **1992**, *43*, 437.
(88) Zhou, W. B., Thorsten; Ivanova, Valentina; Kolb, Dieter M. *Langmuir* **2004**, *20*, 4590-4595.
(89) Zamborini, F. P.; Crooks, R. M. *Langmuir* **1998**, *14*, 3279-3286.

(90) Vericat, C.; Vela, M. E.; Salvarezza, R. C. *Physical Chemistry Chemical Physics* **2005**, *7*, 3258-3268.
(91) Kato, K. *Encyclopedia of Biomaterials and Biomedical Engineering* **2004**, *2*, 1331-1339.
(92) Schreiber, F. *Progress in Surface Science* **2000**, *65*, 151-256.
(93) Buess-Herman, C. *Progress in Surface Science* **1994**, *46*, 335-375.
(94) Porter, M. D.; Bright, T. B.; Allara, D. L.; Chidsey, C. E. D. *Journal of the American Chemical Society* **1987**, *109*, 3559-3568.
(95) Ulman, A. *Characterization of organic thin films*; Butterworth-Heinemann: Boston, 1995.
(96) Campuzano, S.; Pedrero, M.; Montemayor, C.; Fatas, E.; Pingarron, J. M. *Journal of Electroanalytical Chemistry* **2006**, *586*, 112-121.
(97) Finklea, H. O.; Snider, D. A.; Fedyk, J.; Sabatani, E.; Gafni, Y.; Rubinstein, I. *Langmuir* **1993**, *9*, 3660-3667.
(98) Finklea, H. O.; Snider, D. A.; Fedyk, J. *Langmuir* **1990**, *6*, 371-376.
(99) Scharf, J.; Strehblow, H.-H.; Zeysing, B.; Terfort, A. *Journal of Solid State Electrochemistry* **2001**, *5*, 396-401.
(100) Sawaguchi, T. M., F.; Taniguchi, I. *Langmuir* **1998**, *14*, 3565.
(101) Szucs, A. H., G. D.; Bockris, J. O'M *Electrochimica Acta* **1992**, *37*, 403.
(102) Fedurco, M. *Coordination Chemistry Reviews* **2000**, *209*, 263-331.
(103) Lio, A.; Charych, D. H.; Salmeron, M. *Journal of Physical Chemistry B* **1997**, *101*, 3800-3805.
(104) Kaefer, D.; Witte, G.; Cyganik, P.; Terfort, A.; Woell, C. *Journal of the American Chemical Society* **2006**, *128*, 1723-1732.
(105) Ruiz, F. H. S., E.; Inestrosa, N. C. *Biochem. Biophys. Res. Commun.* **2000**, *269*, 491-495.
(106) Meng, R., University of Pittsburgh, Pittsburgh, 2006.
(107) Widrig, C. A.; Chung, C.; Porter, M. D. *Journal of Electroanalytical Chemistry and Interfacial Electrochemistry* **1991**, *310*, 335-359.
(108) Walczak, M. M.; Popenoe, D. D.; Deinhammer, R. S.; Lamp, B. D.; Chung, C.; Porter, M. D. *Langmuir* **1991**, *7*, 2687-2693.